Detecting noise with shot noise using on-chip photon detector

Y. Jompol, P. Roulleau, T. Jullien, B. Roche, I. Farrer, D. A. Ritchie, D. C. Glattli

nature COMMUNICATIONS

ARTICLE

Received 20 Jun 2014 | Accepted 16 Dec 2014 | Published 27 Jan 2015

DOI: 10.1038/ncomms7130

Detecting noise with shot noise using on-chip photon detector

Y. Jompol[1,*,†], P. Roulleau[1,*], T. Jullien[1], B. Roche[1], I. Farrer[2], D.A. Ritchie[2] & D.C. Glattli[1]

The high-frequency radiation emitted by a quantum conductor presents a rising interest in quantum physics and condensed matter. However, its detection with microwave circuits is challenging. Here, we propose to use the photon-assisted shot noise for on-chip radiation detection. It is based on the low-frequency current noise generated by the partitioning of photon-excited electrons and holes, which are scattered inside the conductor. For a given electromagnetic coupling to the radiation, the photon-assisted shot noise response is shown to be independent on the nature and geometry of the quantum conductor used for the detection, up to a Fano factor, characterizing the type of scattering mechanism. Ordered in temperature or frequency range, from few tens of mK or GHz to several hundred of K or THz respectively, a wide variety of conductors can be used like Quantum Point Contacts (this work), diffusive metallic or semi-conducting films, graphene, carbon nanotubes and even molecule, opening new experimental opportunities in quantum physics.

[1] Nanoelectronics Group, Service de Physique de l'Etat Condense, IRAMIS/DSM (CNRS UMR 3680), CEA Saclay, F-91191 Gif-sur-Yvette, France. [2] Semiconductor Physics group, Cavendish Laboratory, University of Cambridge, J.J. Thomson Avenue, Cambridge CB3 0HE, UK. * These authors contributed equally to this work. † Present address: Department of Physics, Mahidol University, Bangkok, Thailand. Correspondence and requests for materials should be addressed to P.R. (email: preden.roulleau@cea.fr).

Using quantum conductors to detect high-frequency radiations is very promising[1–5]. However, it faces some fundamental issues. In particular, the important mismatch between the quantum conductor impedance ($\sim h/e^2$) and the circuit impedance (typically 50 Ω) strongly limits the sensitivity. Recent realizations of on-chip quantum detection[6–12] have circumvented this issue using spatially close detectors with larger impedance providing high sensitivity up to high frequency. On-chip detectors have been realized using GaAs/AlGaAs two-dimensional electron gas (2DEG)-patterned quantum dots[8,9] and Aluminium or Niobium SIS junctions[6,10–12]. The photon response of quantum dots depends on an energy scale set by their geometry, and that of superconducting junctions is limited by a characteristic energy gap and both systems show tunnel resistance variability. Regarding bolometric detectors their efficiency depends on the phonon relaxation time, requires low temperature and shows slow response time.

In this letter, we propose an on-chip radiation detection based on photo-assisted shot noise (PASN). When a quantum conductor is subjected to a time-dependent drain-source voltage, electrons and holes are created which then scatter inside the conductor[13–16]. Their partitioning between source and drain contacts leads to a current noise called PASN. Remarkably, there is a simple link between PASN and the incident radiation power up to a noise Fano factor characterizing the statistics of partitioning. This simple link is better understood if we remark that PASN is the quantum manifestation of the rectification property of ordinary shot noise[17–20], which is proportional to the absolute value of the drain-source voltage.

Results

Photon detection principle. Figure 1 shows the principle of the on-chip detection. It consists of two separate excitation and measurement circuit lines etched in a high-mobility 2DEG. Each line involves two quantum point contacts (QPCs) in series. On the upper line, the left QPC is the high-frequency emitter. When biased by the dc voltage V_{ds}^{E}, it generates shot noise up to the frequency eV_{ds}^{E}/h (refs 19,21). The right QPC tuned on a conductance plateau acts as a stable series resistance R_S^E converting current noise into voltage noise. In the lower line, the left QPC is the detector. In series with the right QPC, also tuned on a resistance plateau R_S^D, it experiences the emitter line voltage fluctuations via the coupling capacitance C_C up to the cutoff frequency f_{max} (ref. 22; Supplementary Fig. 1). The number of electron-hole pairs generated in the detector line is a direct function of the radiated noise power integrated up to frequency $\min(eV_{ds}^{E}/h, f_{max})$ (Supplementary Discussion 1 and Supplementary Fig. 2). Their scattering by the QPC detector generates a low-frequency PASN, which is measured. f_{max} depends on all QPC resistances and on the self-capacitance C_{self} of the 2DEG part between the QPCs in series.

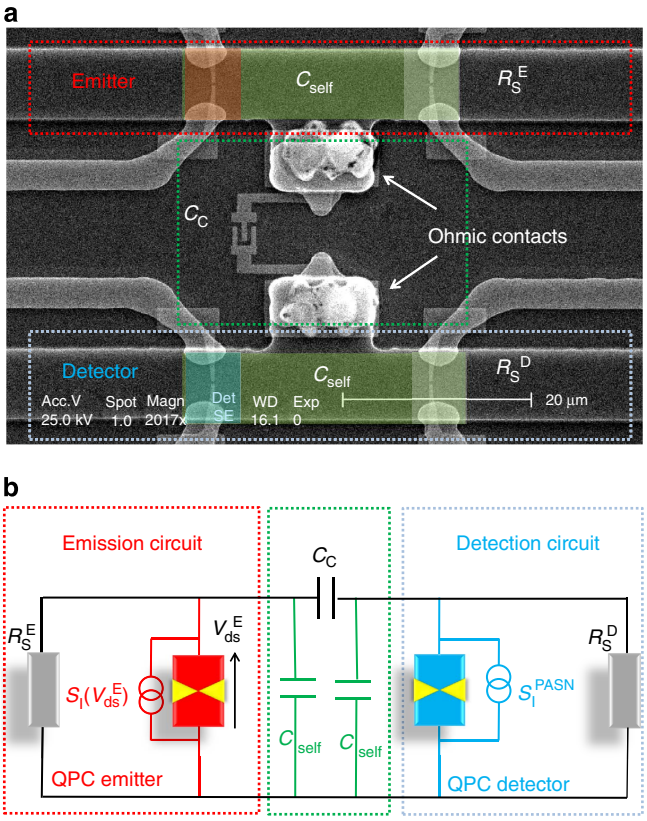

Figure 1 | Device structure. (**a**) Scanning electron microscope view of the sample. The scale bar represents a 20 µm length. Two independent circuit lines defined by wet-chemical etching of the 2DEG are coupled via the capacitance C_C. On the upper line are patterned two QPCs in series: the QPC emitter (in red), and the QPC series resistor (in white) tuned on a plateau. On the lower line, the QPC detector is coloured in blue. (**b**) Equivalent circuit. In red, the emitter line is coupled via the coupling capacitance C_C to the detector line in blue. The self capacitances C_{self} have been added that model the capacitance of each line between the two QPCs to the ground.

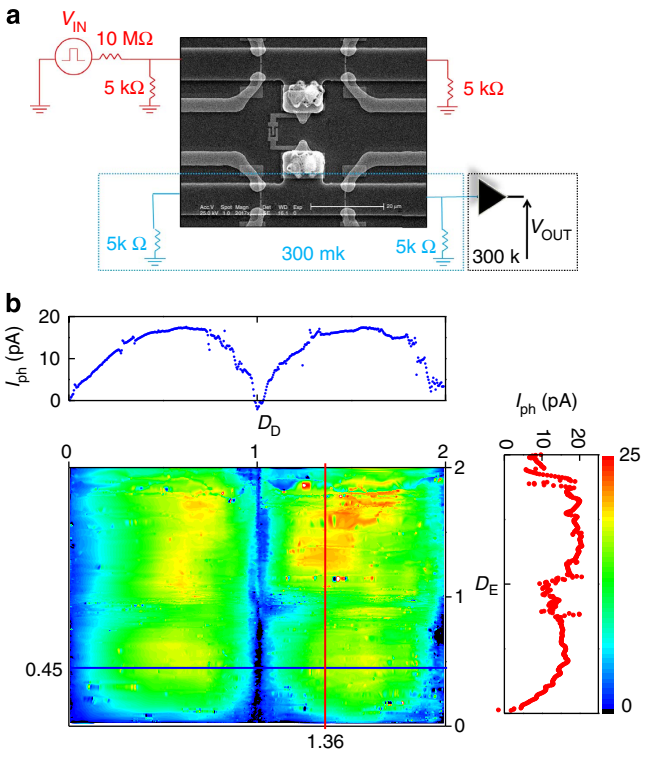

Figure 2 | Photocurrent measurement. (**a**) Schematic representation of the experimental set-up for the photocurrent measurement. The scale bar represents a 20 µm length. The QPC emitter is excited by a sine wave function $V_{pp} \sim 460$ µV at 174 Hz. Resistances of 5 kΩ are used as current to voltage converters. By measuring the output voltage V_{out} after the amplifier (black triangle in the figure), with the excitation source as a reference signal, we can extract the photocurrent. (**b**) The photocurrent as a function of the total transmissions D_D (x axis) and D_E (y axis). On the upper graph is represented the photocurrent as a function of D_D (D_E tuned to 0.45). The right graph shows the photocurrent as a function of D_E (D_D tuned to 1.36).

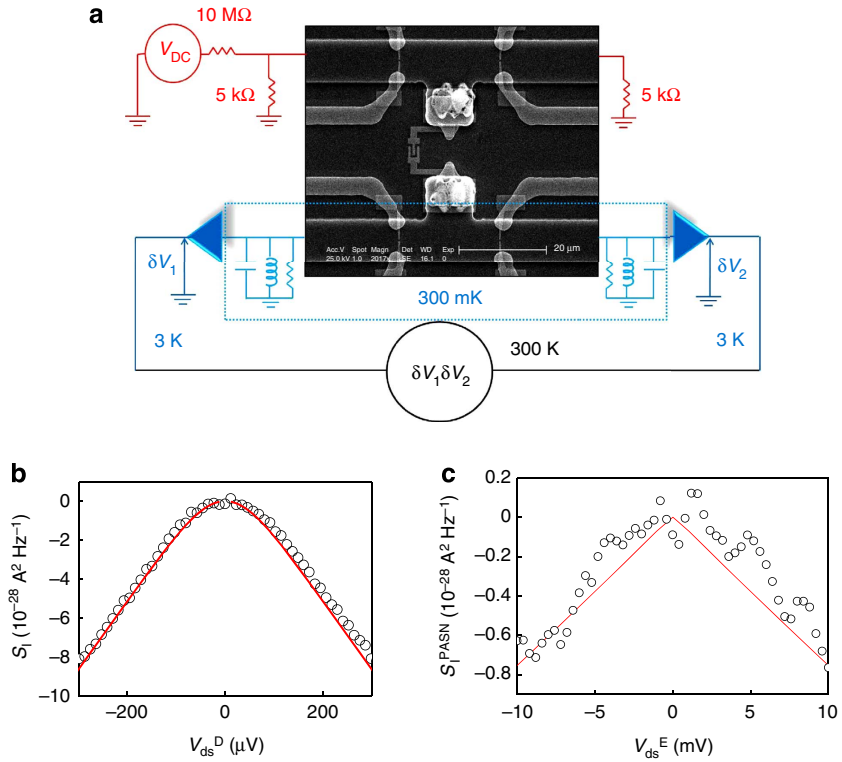

Figure 3 | PASN measurement. (**a**) Schematic representation of the experimental set-up for the PASN measurement. The QPC emitter being biased emits shot noise. Because of the capacitive coupling between the emitter and detector line, high-frequency voltage fluctuations are transferred in the detector line, generating PASN. Shot noise measurements are done by converting the current fluctuations into the voltage fluctuations (noted δV_1 and δV_2) across a parrallel inductor-capacitor resonant circuit (RLC circuit), cooled at 300 mK using 3 MHz resonant frequency and 300 kHz typical bandwidth. Homemade cryogenic amplifiers, with ultra-low input voltage noise (0.2 nV/$\sqrt{Hz}$) and located on the 3 K stage, amplify the voltage fluctuations. Using fast acquisition card and Fast Fourier Transform, the voltage noise cross-correlation $\langle \delta V_1 \delta V_2 \rangle$ is computed in real time. Then $\langle \delta V_1 \delta V_2 \rangle$ is converted into a current shot noise S_I. (**b**) Measured excess shot noise S_I (thermal noise being subtracted) as a function of dc voltage V_{ds}^D across the QPC detector, when the QPC series resistor is opened and the transmission is tuned to 0.17. (**c**) Measured PASN S_I^{PASN} as function of the V_{ds}^E accross the QPC emitter. QPC emitter and detector are tuned at $D_D = D_E = 0.5$. Both series resistances are tuned on the first plateau.

To understand the photon detection principle, let us first assume that the detector line is excited by a coherent radiation at frequency $\Omega/2\pi$ such that $V_{ds}^E(t) = V_{ac}\cos(\Omega t)$. Electrons in the detector line can absorb l photons of energy $E_l = l\hbar\Omega$ by creating an electron-hole pair with a probability $P(E_l) = |J_l(eV_{ac}/\hbar\Omega)|^2$, with J_l the lth Bessel function. Electrons and holes are independently and randomly partitioned by the QPC detector between left and right contacts. This generates a PASN whose low-frequency spectral density of current fluctuations S_I^{PASN} is given by[13–16]:

$$S_I^{PASN} = \frac{2e^2}{h}\left[4k_B T_e \sum_n D_{D,n}^2 + 2\sum_n D_{D,n}(1-D_{D,n}) \sum_{l=-\infty}^{l=+\infty} E_l P(E_l) \coth\frac{E_l}{2k_B T_e}\right] \quad (1)$$

with T_e the electronic temperature and $D_{D,n}$ the transmission of the nth electronic mode contributing to the QPC detector conductance G_D, $n = 1, 2,....$ We introduce the Fano factor F defined as $F = \sum_n D_{D,n}(1-D_{D,n})/\sum_n D_{D,n}$. For weak ac voltage $eV_{ac} \ll \hbar\Omega$ and zero temperature, a direct relation can be established between the radiation power $P_{rad} = V_{ac}^2/2Z_{rad}$ and the current noise: $S_I^{PASN} \simeq 2G_D F(Z_{rad}e^2/\hbar)P_{rad}/\Omega$, where Z_{rad} is the radiation impedance assumed smaller than the QPC detector conductance G_D and F the Fano factor. In equation (1), the sum over the energies E_l gives the probability to generate electron-hole pairs. This probability only depends on the excitation and not on the details of the detector.

From equation (1), it is clear that the maximum PASN will be obtained for total transmission $D_D = \sum_n D_{D,n} = k + 1/2$, k an integer. In addition to shot noise, a photon-assisted dc current I_{ph} is generated when considering the (weak) energy dependence of the QPC transmission:

$$I_{ph} = \frac{2e}{h}\int d\epsilon\left(-\frac{\partial f}{\partial \epsilon}\right)\left(\sum_n \frac{\partial D_{D,n}}{\partial \epsilon}\right)\sum_{l=-\infty}^{l=+\infty} E_l^2 P(E_l) \quad (2)$$

$f(\epsilon)$ is the equilibrium Fermi distribution. Photocurrent requires the energy dependence of the QPC. After photons absorption, electron-hole pairs are generated. As electrons and holes do not have the same transmission, a net DC current is induced. The energy dependence of transmission is strongly sample dependent and makes the photocurrent response not universal. On the contrary, the PASN response only depends on the Fano factor, which can be measured from conductance for a single-mode QPC, or is even universal, that is, 1/3, for a diffusive conductor. Modelling the QPC transmission with a saddle point potential[23,24], it can be shown that $\frac{\partial D_{D,n}}{\partial \epsilon} \propto D_{D,n}(1-D_{D,n})$: maximum photocurrents will be also obtained at half-integer D_D.

In the present case, the excitation is not coherent but due to random fluctuations of the QPC detector drain-source voltage that originates from the capacitive coupling with the noisy QPC

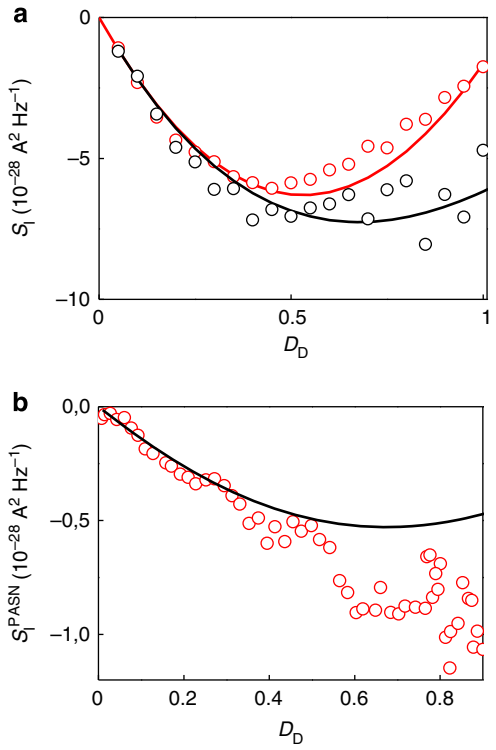

Figure 4 | Transmission dependence of the PASN. (**a**) Red dots: measured shot noise as a function of D_D for an opened series QPC together with our theoretical model (red solid line). Black dots: same measurement with the series QPC tuned on a plateau. The non-zero value of tefhe noise for $D_D = 1$ results from heating effect. In both cases, $V_{ds}^{D} = 150\,\mu V$. The noise due to the heating of the series resistance has been subtracted. (**b**) Red dots: measured PASN as function of D_D for the series QPC tuned on the first plateau and a fixed $D_E \sim 0.5$ (theoretical prediction represented by a black solid line). The applied DC bias is $V_{ds}^{E} = 6\,mV$.

emitter. The above expressions can be generalized, giving the PASN as:

$$S_I^{PASN} = \frac{2e^2}{h}\left[4k_B T_e \sum_n D_{D,n}^2 + 2\sum_n D_{D,n}(1-D_{D,n})\int EP(E)\coth\frac{E}{2k_B T_e}dE\right] \quad (3)$$

and the photocurrent:

$$I_{ph} = \frac{2e}{h}\int d\epsilon\left(-\frac{\partial f}{\partial \epsilon}\right)\left(\sum_n \frac{\partial D_{D,n}}{\partial \epsilon}\right)\int E^2 P(E)dE \quad (4)$$

The generalized probability distribution $P(E)$ is similar to the $P(E)$ function used in the dynamical Coulomb blockade theory (Supplementary Discussion 2). It is a direct function of the radiation power to be detected, which as a shot noise itself is maximum for $D_E = 0.5$.

Photocurrent measurement. We first focus on the photocurrent whose measurement set-up is described in Fig. 2a. Source V_{in} leads to a current in the upper line and to the voltage difference V_{ds}^{E} across the emitter. The resulting shot noise induces a photocurrent I_{ph} in the detector. We modulate V_{in} at frequency 174 Hz and detect the induced photocurrent using lock-in techniques. Series resistances are tuned on a plateau for each line, whereas the emitter and detector transmissions are varied. Following the saddle point potential model of a QPC[23,24], the transmission of the nth mode can be written $D_{D,n}(V_g) = 1/(1+e^{2\pi(V_0 - V_g)}/V_{g,n})$, where $V_{g,n}$ is related to the negative curvature of the saddle point potential. The photocurrent is given by (Supplementary Discussion 3):

$$I_{ph} = \frac{e}{h}\frac{1}{\Delta}\frac{k_B T_E^* e^2}{C_{self}}\sum_n \frac{2\pi}{V_{g,n}} D_{D,n}(1-D_{D,n}) \quad (5)$$

$V_{g,n}$ and the lever arm $\Delta = \partial\epsilon/\partial V_g$ are extracted from a study of the differential QPC conductance versus gate and bias voltages. We have introduced T_E^* as the effective noise temperature of the circuit, which, up to a coupling factor, includes a combination of the shot noise temperature of the emitter: $(1-D_E)\frac{eV_{ds}^{E}}{2k_B}$ plus other equilibrium thermal noise contributions of the circuit surrounding the detector QPC. The coupling capacitance C_C appears in T_E^* via the transimpedance of the system, which characterizes the strength of the coupling. Considering the geometry of C_C, independent simulations give $C_C \sim 1$ fF.

The colour plot in Fig. 2b shows the measured photocurrent as a function of the emitter and detector transmissions D_E and D_D, up to two transmitting orbital electronic modes. Above the colour plot, the photocurrent is plotted as a function of D_D for a fixed value of $D_E \sim 0.45$. As expected, it is maximum for half transmission of the emitter electronic modes and vanishes for integer transmission. These measurements have been found essential for a fine calibration of the electrical circuit and for complementary characterization of the PASN effect (Supplementary Fig. 3).

PASN detection. We now consider PASN measurements. The cross-correlation noise measurement set-up is described in Fig. 3a. To characterize the detector line, the QPC detector transmission is set to $D_D = 0.17$, whereas a dc bias is applied on the detector line. The resulting shot noise measured, black dots in Fig. 3b, perfectly agrees with the theory in red solid line. We extract an electronic temperature $T_e = 310$ mK close to the fridge temperature $T = 300$ mK. Then, we turn off the applied bias on the detector line and the QPC emitter is biased and also tuned at transmission $D_E = 0.5$. Both series resistances are tuned on the first plateau. Because of the coupling capacitance, voltage fluctuations are reported on the detector line. The only dc current flowing through the detector line being the weak dc photocurrent, no detectable transport shot noise is expected. However, we detect some noise, confirming that the PASN detection works as illustrated in Fig. 3c, black circle. The detected PASN, $\Delta S_I^{PASN,D}$, is expected to be (Supplementary Discussion 4):

$$\Delta S_I^{PASN,D} \simeq -\frac{4e^2}{h} D_D(1-D_D)\frac{e^2}{C_{self}}\frac{T_E^*}{6T_e} \quad (6)$$

Here, considering $P(E)$ takes only important values for $E \ll k_B T_e$, a low-energy expansion of equation (3) has been made. The $T_E^*(V_{ds}^{E})/C_{self}$ amplitude compatible with the detector geometry (estimated $C_{self} = 3$ fF and $C_C = 0.9$ fF) and obtained from photocurrent measurements can now be compared with the noise measurement. The theoretical prediction (red solid line) following equation (6) also includes an additional term because of heating effect. We discuss this point in the following.

We open the series QPC of the detector line such that the current-to-voltage fluctuation conversion is now mediated by the smaller resistance of the long resistive mesa. Then we apply a fixed bias V_{ds}^{D} and sweep the detector transmission (red circles in Fig. 4a). As expected, the shot noise is maximum for $D_D = 0.5$ and cancels for $D_D = 1$. The slight disagreement with the theoretical prediction (red solid line) around $D_D \sim 0.7$ reveals a weak '0.7' anomaly[25–28]. Then we tune the series QPC on its first plateau and repeat the same experiment (black circles). Surprisingly, the

shot noise does not cancel anymore for $D_D = 1$. To understand it, we must consider heating effects (Supplementary Discussion 5). As the size of the QPC is much smaller than the electron-phonon relaxation length, there is a temperature gradient from the QPC to the ohmic contacts assumed to be at the base temperature of the fridge. Combining Joule heating together with the Wiedemann–Franz law, we obtain[17] (Supplementary Fig. 4):

$$T_e^2(V_{ds}) = T_{fridge}^2 + \frac{24}{\pi^2}\frac{G}{G_m}\left(1+\frac{2G}{G_m}\right)\left(\frac{eV_{ds}}{2k_B}\right)^2 \qquad (7)$$

with G_m the total conductance linking the QPC to the ohmic contacts and T_{fridge} the base temperature. Considering this effect, a QPC tuned on a plateau will not be noiseless anymore. We find a good agreement with measurements, black solid line.

We now apply $V_{ds}^E = 6$ mV on the emitter line, fixing $D_E \sim 0.5$ to get the maximum emitted signal. In Fig. 4b, the PASN is measured as a function of D_D. The non-zero value of the shot noise for $D_D = 1$ results from the similar heating effect (Supplementary Fig. 5).

Discussion

The agreement between theory and experimental data confirms our good understanding of the 'on-chip' detection mechanism: *both photocurrent and PASN result from the same photon-assisted effect*. As the photon current detector is based on the energy dependence of the transmission, which is strongly geometry dependent, it raises the question of the use of such a detector based on a common calibration. On the contrary, PASN detection only depends on the transmission. For metallic diffusive system, the Fano factor is even constant 1/3 (ref. 29) and such a detector could be used on a large scale. Regarding the photodetection efficiency, there is a competition between the direct coupling C_C of the two lines and the shortcut to the ground characterized by C_{self}. In the future, we will increase the number of fingers of the interdigitated C_C and reduce the area between the QPC to lower C_{self}, and therefore reach the most efficient regime where $C_{self} \ll C_C$.

To conclude, we have described a way of detecting high-frequency voltage fluctuations based on PASN measurement and seconded by photocurrent measurement. If the latter depends on the details of the mesoscopic conductor used, PASN is universal up to a noise Fano factor. The PASN approach for noise or photon radiation detection can be applied to other systems. This technique offers the possibility to probe mesoscopic properties at very high frequency (GHz and THz) of various materials (GaAs, graphene, carbon nanotube).

Methods

Emitter and detector lines were patterned using e-beam lithography on a high-mobility 2DEG formed at the GaAs/$Ga_xAl_{1-x}As$ heterojunction. The 2DEG, located at a depth of 100 nm below the surface, has a density of $1.8\times10^{11}\,cm^{-2}$ and mobility of $2.69\times10^6\,cm^2\,V^{-1}\,s^{-1}$. Measurements were performed in cryogen-free ^{3}He cryostat at 300 mK (base temperature).

References

1. Aguado, R. & Kouwenhoven, L. P. Double quantum dots as detectors of high-frequency quantum noise in mesoscopic conductors. *Phys. Rev. Lett.* **84,** 1986 (2000).
2. Zazunov, A., Creux, M., Paladino, E., Crpieux, A. & Martin, T. Detection of finite-frequency current moments with a dissipative resonant circuit. *Phys. Rev. Lett.* **99,** 066601 (2007).
3. Beenakker, C. W. J. & Schomerus, H. Antibunched photons emitted by a quantum point contact out of equilibrium. *Phys. Rev. Lett.* **93,** 096801 (2004).
4. Zakka-Bajjani, E. *et al.* Experimental determination of the statistics of photons emitted by a tunnel junction. *Phys. Rev. Lett.* **104,** 206802 (2010).
5. Trauzettel, B., Safi, I., Dolcini, F. & Grabert, H. Appearance of fractional charge in the noise of non-chiral Luttinger liquids. *Phys. Rev. Lett.* **92,** 226405 (2004).
6. Basset, J. *et al.* Measurement of quantum noise in a carbon nanotube quantum dot in the Kondo Regime. *Phys. Rev. Lett.* **108,** 046802 (2012).
7. Delbecq, M. R. *et al.* Coupling a Quantum dot, fermionic leads, and a microwave cavity on a chip. *Phys. Rev. Lett.* **107,** 256804 (2011).
8. Gustavsson, S. *et al.* Frequency-selective single-photon detection using a double quantum dot. *Phys. Rev. Lett.* **99,** 206804 (2007).
9. Onac, E. *et al.* Using a quantum dot as a high-frequency shot noise detector. *Phys. Rev. Lett.* **96,** 176601 (2006).
10. Deblock, R., Onac, E., Gurevich, L. & Kouwenhoven, L. P. Detection of quantum noise from an electrically driven two-level system. *Science* **301,** 203 (2003).
11. Billangeon, P. M., Pierre, F., Bouchiat, H. & Deblock, R. Emission and absorption asymmetry in the quantum noise of a Josephson junction. *Phys. Rev. Lett.* **96,** 136804 (2006).
12. Basset, J., Bouchiat, H. & Deblock, R. Emission and absorption quantum noise measurement with an on-chip resonant circuit. *Phys. Rev. Lett.* **105,** 166801 (2010).
13. Lesovik, G. B. & Levitov, L. S. Noise in an ac biased junction: Nonstationary Aharonov-Bohm effect. *Phys. Rev. Lett.* **72,** 538 (1994).
14. Pedersen, M. H. & Büttiker, M. *Phys. Rev. B* **58,** 12993 (1998).
15. Schoelkopf, R. J., Kozhevnikov, A. A., Prober, D. E. & Rooks, M. J. Observation of 'photon-assisted' shot noise in a phase-coherent conductor. *Phys. Rev. Lett.* **80,** 2437 (1998).
16. Reydellet, L.-H., Roche, P., Glattli, D. C., Etienne, B. & Jin, Y. Quantum partition noise of photon-created electron-hole pairs. *Phys. Rev. Lett.* **90,** 176803 (2003).
17. Kumar, A., Saminadayar, L., Glattli, D. C., Jin, Y. & Etienne, B. Experimental test of the quantum shot noise reduction theory. *Phys. Rev. Lett.* **76,** 2778 (1996).
18. Reznikov, M., Heiblum, M., Shtrikman, H. & Mahalu, D. Temporal correlation of electrons: suppression of shot noise in a ballistic quantum point contact. *Phys. Rev. Lett.* **75,** 3340 (1995).
19. Lesovik, G. B. Excess quantum noise in 2D ballistic point contacts. *JETP Lett.* **49,** 594 (1989).
20. Blanter, Y. M. & Büttiker, M. Shot noise in mesoscopic conductors. *Phys. Rep.* **336,** 1 (2000).
21. Zakka-Bajjani, E. *et al.* Experimental test of the high-frequency quantum shot noise theory in a quantum point contact. *Phys. Rev. Lett.* **99,** 236803 (2007).
22. Hashisaka, M. *et al.* Bolometric detection of quantum shot noise in coupled mesoscopic systems. *Phys. Rev. B* **78,** 241303(R) (2008).
23. Büttiker, M. Quantized transmission of a saddle-point constriction. *Phys. Rev. B* **41,** 7906(R) (1990).
24. Kemble, E. C. A contribution to the theory of the B. W. K. method. *Phys. Rev.* **48,** 549 (1938).
25. Thomas, K. J. *et al.* Possible spin polarization in a one-dimensional electron gas. *Phys. Rev. Lett.* **77,** 135 (1996).
26. Roche, P. *et al.* Fano factor reduction on the 0.7 conductance structure of a ballistic one-dimensional wire. *Phys. Rev. Lett.* **93,** 116602 (2004).
27. Reilly, D. J., Zhang, Y. & DiCarlo, L. Phenomenology of the 0.7 conductance feature. *Physica E* **34,** 27 (2006).
28. DiCarlo, L. *et al.* Shot-noise signatures of 0.7 structure and spin in a quantum point contact. *Phys. Rev. Lett.* **97,** 036810 (2006).
29. Beenakker, C. W. & Büttiker, M. Suppression of shot noise in metallic diffusive conductors. *Phys. Rev. B* **46,** 1889(R) (1992).

Acknowledgements

The ERC Advanced Grant 228273 is acknowledged. We are grateful to P. Jacques for experimental support.

Author contributions

D.C.G. designed the project. Y.J., P.R., T.J. and B.R. performed the experiments and analysed data. P.R. and D.C.G. wrote the manuscript. Y.J and, P.R. set-up the measurement system. Y.J. fabricated the sample. I.F. and D.A.R. grew the wafer.

Additional information

Supplementary Information accompanies this paper at http://www.nature.com/naturecommunications

Competing financial interests: The authors declare no competing financial interests.

Reprints and permission information is available online at http://npg.nature.com/reprintsandpermissions/

How to cite this article: Jompol, Y. *et al.* Detecting noise with shot noise using on-chip photon detector. *Nat. Commun.* 6:6130 doi: 10.1038/ncomms7130 (2015).